Structural Engineering and Mechanics, Vol. 24, No. 1 (2006) 91-105
DOI: http://dx.doi.org/10.12989/sem.2006.24.1.091

Post-earthquake capacity evaluation of R/C buildings based on pseudo-dynamic tests

Dae-eon Kang† and Waon-ho Yi‡

ESnS Structure Research Center, Department of Architectural Engineeing, Kwangwoon University, Seoul, Korea

(Received January 14, 2005, Accepted April 17, 2006)

Abstract. In this paper, post-earthquake capacity evaluation method of reinforced concrete buildings was studied. Substructure pseudo-dynamic test and static loading test of first story column in a four-story R/C building was carried out in order to investigate the validity of the evaluation method proposed in the Damage Assessment Guideline (JBDPA 2001). In pseudo-dynamic test, different levels of damage were induced in the specimens by pre-loading, and input levels of seismic motion, at which the specimens reached to the ultimate stage, were examined. From the experimental result, no significant difference in damage levels such as residual crack width between the specimens under static and pseudo-dynamic loading was found. It is shown that the seismic capacity reduction factors η can provide a reasonable estimation of post-earthquake seismic capacity of R/C buildings suffered earthquakes.

Keywords: post-earthquake capacity; R/C; pseudo-dynamic test; damage levels; seismic capacity reduction factor.

1. Introduction

In damage investigation of building structures suffering from earthquake, estimation of residual seismic capacity is essential in order to access the safety of the building against aftershocks and to judge the necessity of repair and restoration. Bunno *et al.* (2000) have proposed an evaluation method for post-earthquake seismic capacity of reinforced concrete (R/C) buildings based on the residual energy dissipation capacity of structural. The proposed method was adopted in the Japanese "Damage Level Classification Standard" revised in 2001 (JBDPA 2001). In the Damage Assessment Guideline, the seismic capacity reduction factor η was defined based on absorbable energy in a structural member, which was evaluated from an idealized monotonic load-deflection curve and accordingly the effect of cyclic behavior under seismic vibration was not taken into account. Therefore substructure pseudo-dynamic test of first story column in a four-story R/C building was carried out in order to investigate the validity of the proposed evaluation method for post-earthquake seismic capacity. Residual seismic capacity ratio based on pseudo-dynamic test, R_{dyn}, was defined by the ratio of the intensity of ultimate ground motion after damage to that before an earthquake (Fig. 1). The ultimate ground motion was defined as a ground motion necessary to

† Research Professor, Corresponding author, E-mail: kde0898@hanmail.net
‡ Professor

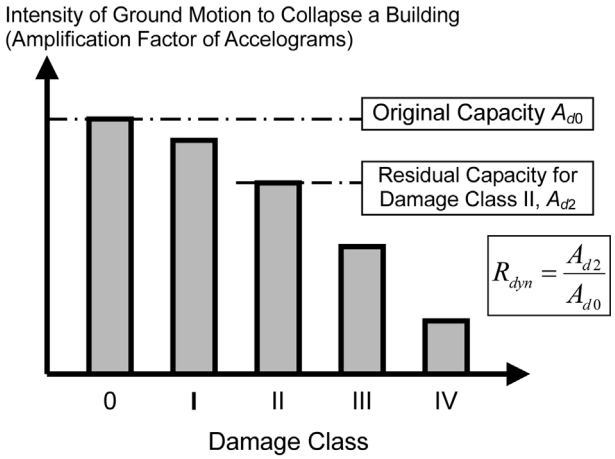

Fig. 1 Residual seismic capacity ratio based on seismic response R_{dyn}

induce ultimate limit state in a member structure and the member would collapse.

$$R_{dyn} = \frac{A_{di}}{A_{d0}} \tag{1}$$

where, A_{d0} : intensity of ultimate ground motion before an earthquake (damage class 0)
A_{di} : intensity of ultimate ground motion after damage (damage class "*i*")

2. Damage evaluation guideline

First, structural damage is surveyed and damage of structural members is classified in the most severely damaged story. The residual seismic capacity ratio index R is then calculated and damage rating of the building structure, i.e., [slight], [minor], [moderate], [severe], and [collapse] is made. Necessary actions are finally determined comparing the intensity of the ground motion at the building site, building damage rating, and required seismic capacity against a future earthquake.

Table 1 Damage class for RC structural members

Damage class	Observed damage on structural members
I	Visible narrow cracks are found (Crack width is less than 0.2 mm)
II	Visible clear cracks on concrete surface (Crack width is about 0.2-1 mm)
III	Local crush of covering concrete Remarkable wide cracks (Crack width is about 1-2 mm)
IV	Remarkable crush of covering concrete with exposed reinforcing bars Spalling off of covering concrete (Crack width is more than 2 mm)
V	Buckling of reinforcing bars Cracks in core concrete Visible vertical and/or lateral deformation in columns and/or walls Visible settlement and/or inclination of the building

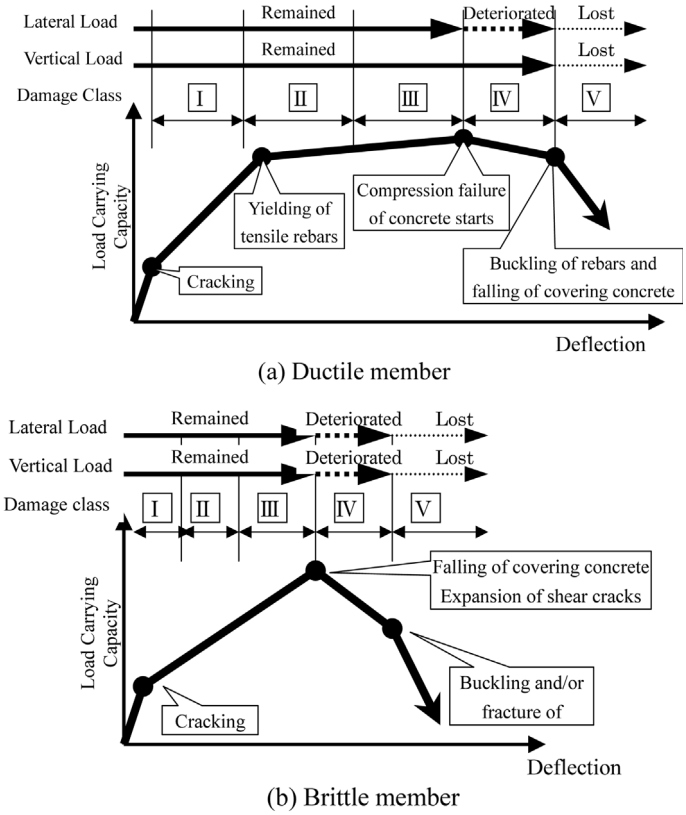

Fig. 2 Lateral load – deflection relationships and damage class

2.1 Damage classification of structural members

Damage of columns and shear walls is classified based on the damage definition shown in Table 1. As was reported in the past earthquake in Japan, typical damage is generally found in vertical members, and the Guideline is essentially designed to identify and classify damage in columns and walls rather than in beams. Columns and walls are classified in one of five categories I through V as defined in Table 1. Fig. 2 schematically illustrates the load carrying capacity, load-deflection curve, and member damage class.

2.2 Residual seismic capacity ratio index R

A residual seismic capacity ration index R, which corresponds to building damage, is defined by as the ratio of seismic capacity after damage to that before an earthquake (i.e., the ratio of the residual capacity to the original capacity).

$$R = \frac{{}_{D}Is}{Is} \times 100 \tag{2}$$

where, Is: seismic capacity index of structure before earthquake damage

${}_{D}Is$: seismic capacity index of structure considering deteriorated member strength

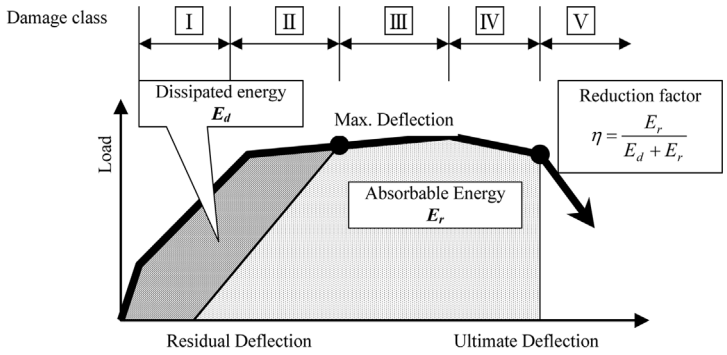

Fig. 3 Definition of seismic capacity reduction factor η

Table 2 Seismic capacity reduction factor η

Damage class	Ductile column	Brittle column	Wall
I	0.95	0.95	
II	0.75	0.6	
III	0.5	0.3	
IV	0.1	0	
V	0	0	

Is-index can be calculated based on the Standard for Seismic Evaluation (JBPDA 2001b), which is most widely applied to evaluate seismic capacity of existing buildings in Japan. The basic concept of the Standard to calculate *Is*-index appears in APPENDIX. The Guideline recommends to calculate ${}_{D}Is$-index for a damaged building in the analogous way for pre-event buildings, considering seismic capacity reduction factor η defined as the ratio of the absorbable hysteretic energy after earthquake to the original absorbable energy of a structural member as illustrated in Fig. 3. Table 2 shows the values of the reduction factor η in the Guideline.

$$\eta = \frac{E_r}{E_t} \tag{3}$$

where, E_d : dissipated energy
E_r : residual absorbable energy
E_t : entire absorbable energy $(E_t = E_d + E_r)$.

${}_{D}Is$-index for a damaged building can be calculated from residual member strength reduced by the reduction factor η and the original member ductility, and then residual seismic capacity ration index R is evaluated.

2.3 Damage rating of building

The residual seismic capacity ratio index R can be considered to represent damage sustained by a building. For example, it may represent no damage when R = 100% (100% capacity is preserved), more serious damage with decrease in R, and total collapse when R = 0% (no residual capacity). To

identify the criteria for damage rating, R values of 145 RC school buildings that suffered 1995 Kobe Earthquake are compared with observed damage and judgments by experts. The Guideline defines the damage rating criteria shown below.

[slight] $95 \leqq R$ (%)
[minor] $80 \leqq R < 95$ (%)
[moderate] $60 \leqq R < 80$ (%)
[severe] $R < 60$ (%)
[collapse] $R \approx 0$

3. Outlines of experiment

3.1 Description of specimens

Four column specimens were tested in this study. The specimen represented an interior column in the first story of an existing 4-storied R/C building as shown in Fig. 4. All specimens have the same

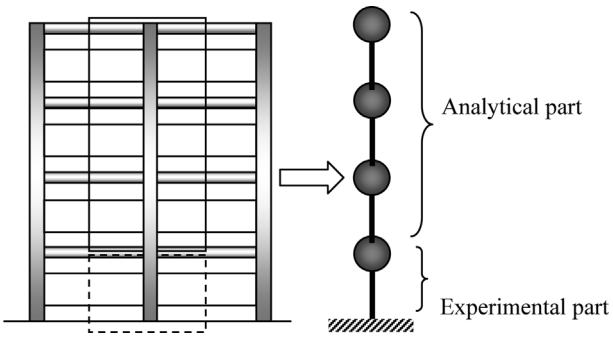

Fig. 4 Objective building and analytical model for pseudo-dynamic test

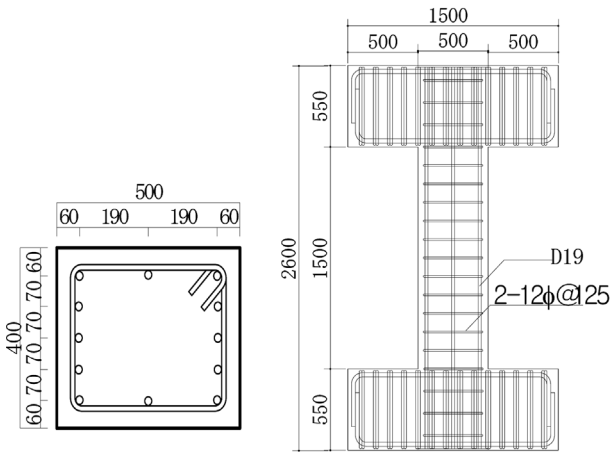

Fig. 5 Dimensions and reinforcements distribution of specimens

Table 3 Dimensions and reinforcements of specimens

$B \times D$	h_0	Longitudinal reinforcement	p_t	Shear reinforcement	p_w	N
400 × 500	1500	10-D19	0.57	2-12ϕ @ 125	0.45	953

h_0: clear height (mm), P_t: tension reinf. ratio (%), P_w: lateral reinf. ratio (%), N: axial load (kN)

Table 4 Material properties of concrete and reinforcements

Concrete		Reinforcements		
σ_y (Mpa)	ε_{cu} (%)	Size and quality	σ_y (Mpa)	ε_y (%)
27.2	0.18	D19	364	0.187
		12ϕ	329	0.161

σ_y: compressive strength, ε_{cu}: strain at the strength, σ_y: yield strength, ε_y: yield strain

dimension and reinforcement. The properties and reinforcing details are shown in Fig. 5 and Table 3. The dimensions of a column section were 40 × 50 cm and shear span-to-depth ratio was 1.5 (150 cm height). Ten D19 bars (nominal diameter of 1.91 cm, nominal area of 2.87 cm^2) were arranged as longitudinal reinforcement. 19ϕ bars (round bar, diameter of 1.9 cm) were arranged as lateral reinforcement with 12.5 cm spacing. Mechanical properties of concrete and reinforcement are shown in Table 4.

3.2 Parameters of experiment

Experimental parameters are shown in Table 5. Three specimens named PSD0, PSD2, and PSD3 were examined by pseudo-dynamic testing. The specimens PSD2 and PSD3 were damaged by pre-loadings. Target initial damage levels for PSD2 and PSD3 were minor damage (damage class II by the Damage Level Classification Standard) and moderate damage (damage class III), respectively. On the other hand, PSD0 was tested with no structural damage. The damaged and undamaged specimens were tested by pseudo-dynamic testing using amplified input seismic motion at which the specimens reached to the ultimate stage. The specimen ST was tested by static loading to compare the failure patterns, damage levels and hysteresis loops with the specimens under pseudo-dynamic testing.

Table 5 Parameters of experiment

	Loading	Initial damage	Damage class*
PSD0	Pseudo-Dynamic	None	0
PSD2		Minor	II
PSD3		Moderate (or Severe)	III
ST	Static	None	0

*Damage Level Classification Standard (JBPDA 2001)

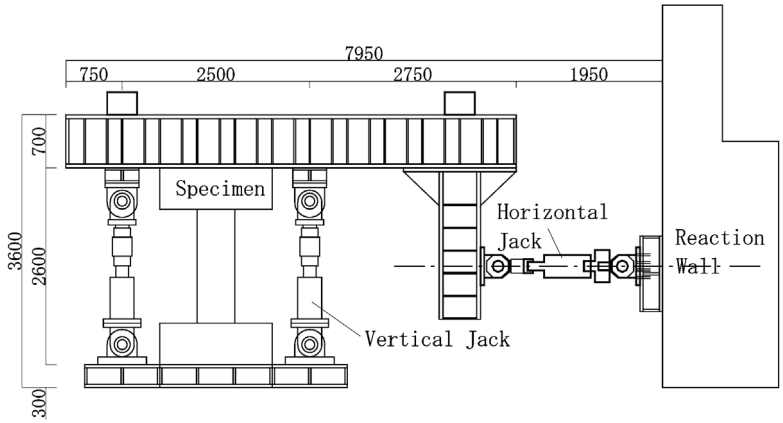

Fig. 6 Testing apparatus

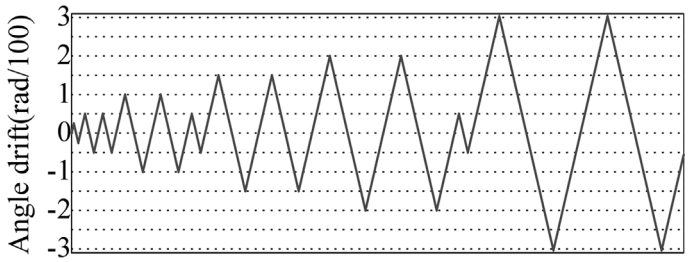

Fig. 7 Loading history of ST specimen

3.3 Test method and loading system

3.3.1 Loading apparatus

Loading apparatus is illustrated in Fig. 6. The specimens were subjected to bending and shear by a horizontal jack. The vertical jacks on both side of the specimen kept the top and bottom stubs and applied constant axial. Fig. 7 shows the loading history, where angle drift is defined as "lateral deformation/column height (1500 mm)". As shown in the figure, the specimen ST was subjected to two cycles at drift angle of 1/200, 1/100, 1/67, 1/50, 1/33 radian after the first cycle at a drift angle of 1/400. It should also be noted that 1/200 loading is imposed after 1/100 and 1/50 to investigate the effect of small amplitude loading after large deformation (i.e., aftershocks). After severe damage is found, the specimen is pushed after to collapse.

3.3.2 Method of pseudo-dynamic test

The specimens PSD0, PSD2 and PSD3 were tested by sub-structure pseudo-dynamic method. The objected building was reduced to a 4-degree-of-freedom system. As shown in Fig. 4, the column specimen represents the first story column and second to fourth stories were analyzed. The specimen was subjected to the target story drift angle which was calculated from step-by-step seismic response analysis of the 4-degree-of-freedom system. Takeda model (Takeda *et al.* 1970) was used as hysteresis model for the analytical parts in seismic response analyses. The crack and

yielding strengths of the specimens are calculated according to the Japanese "Standard for Structural Calculation" (AIJ 1999).

The time integration scheme used in pseudo-dynamic test is unconditionally unstable and is termed the Operator-Splitting (OS) method (Nakashima *et al.* 1999). The OS method does not require any iteration for nonlinear analysis. Time increment of response analysis was 0.005 second and viscous damping matrix was assumed to be proportional to stiffness matrix $[K_y]$ at yielding, which was 2% of natural frequency. In this method, the equations of motion are formulated as follows.

$$Ma_{n+1} + Cv_{n+1} + K^I d_{n+1} + \tilde{r}_{n+1} - K^I \tilde{d}_{n+1} = p_{n+1} \tag{4}$$

$$M = \begin{bmatrix} m_1 & 0 & 0 & 0 \\ 0 & m_2 & 0 & 0 \\ 0 & 0 & m_3 & 0 \\ 0 & 0 & 0 & m_4 \end{bmatrix}, \quad K^I = \begin{bmatrix} k_1 + k_2 & -k_2 & 0 & 0 \\ -k_2 & k_2 + k_3 & -k_3 & 0 \\ 0 & -k_3 & k_3 + k_4 & -k_4 \\ 0 & 0 & -k_4 & k_4 \end{bmatrix}, \quad C = \frac{2\xi_1}{\varpi_1}[K_y]$$

$$m_1 = m_2 = m_3 = m_4 = \frac{1}{4}\frac{W}{g}, \text{ mass of each story}$$

(W (weight of structure) = Axial load = 953 kN, g; the acceleration of gravity)

$$k_1 = k_2 = k_3 = k_4 = 232 \text{ kN/mm}, \text{ stiffness of each story}$$

$$\xi_1 = 0.02, \left| -\varpi_1^2[M] + [K_y] \right| = 0$$

In which K^I is the predictor stiffness matrix of the structure and $\tilde{r}_{n+1}$ is the restoring force vector based on predictor displacements $\tilde{d}_{n+1}$. The displacement and velocity quantities are approximated in the same way as in the constant-average-acceleration method, i.e.,

$$d_{n+1} = \tilde{d}_{n+1} + \frac{\Delta t^2}{4} a_{n+1} \tag{5}$$

$$v_{n+1} = v_n + \frac{\Delta t}{2}(a_n + a_{n+1}) \tag{6}$$

where

$$\tilde{d}_{n+1} = d_n + \Delta t v_n + \frac{\Delta t^2}{4} a_n \tag{7}$$

With this scheme, a test can be conducted as follows. Assuming that the response in step n has been computed, calculate the predictor displacements $\tilde{d}_{n+1}$ with Eq. (7) and impose them on the analytical and experimental substructures, respectively. Measure the restoring forces developed by the specimen and assemble for the entire structure. Substitute $\tilde{r}_{n+1}$ and $\tilde{d}_{n+1}$ into Eq. (4) and solve for d_{n+1} with Eqs. (4) through (7). Repeat the above procedure by setting $n = n + 1$ until the entire response history is obtained.

NS component of JMA (Japan Meteorological agency) KOBE recorded at 1995 Hyogo-ken-nambu Earthquake was adopted for the input ground motion. The input acceleration is shown in Fig. 8. Table 6 shows the target structural damage levels of the specimens and the amplification factors of input ground acceleration for each RUNs, respectively. As mentioned earlier, specimens

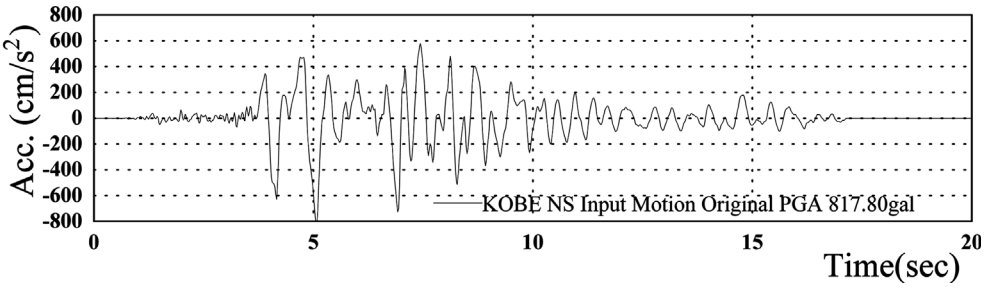

Fig. 8 Acceleration record for input ground motion (JMA Kobe NS)

Table 6 Target structural damage and amplification factor of input acceleration

Specimen	Input	Target damage level	Amplification factor
PSD2	RUN0	II	0.25
	RUN0+		0.41
	RUN1	V	0.41
PSD3	RUN0	III	0.50
	RUN1	V	0.30
PSD0	RUN1	V	0.60

PSD2 and PSD3 were induced structural damage of damage class II and III, respectively, by pre-loading named "RUN0" in order to estimate the residual seismic capacity. Note that additional pre-loading "RUN0+" was applied to specimen PSD2 because the damage level due to the RUN0 remained damage class I. Then all specimens were subjected to amplified input acceleration so that the specimen reached to the ultimate state and failed (damage class V).

4. Test results

4.1 Results of static loading

Fig. 9 shows the observed shear force – lateral displacement relation for specimen ST. Crack pattern was shown in Photo 1. Longitudinal bars yielded at the drift angle of the order of 1/200 after generation of flexural and shear cracks. The process to failure was as follows; i.e., at a drift angle of 1/100 rad., bond splitting cracks along longitudinal bars were observed. The lateral load began to decrease gradually with propagation of bond splitting cracks and, finally, bond splitting failure was observed.

The relationship between the maximum residual crack width and drift angle at the peak of each cycle was shown in Fig. 10. The residual crack widths were measured by crack scale at the moment when the lateral force was unloaded. In the figure, crack width of 0.2, 1, and 2 mm correspond to the borders between the damage classes of the structural members, according to Table 1 (JBDPA 2001). The crack widths were smaller than 0.2 mm, which correspond to the "damage class I (slight damage)", until flexural yielding occurred in a cycle at 1/200 rad. After flexural yielding, the maximum residual crack widths increased markedly with increase in drift angle.

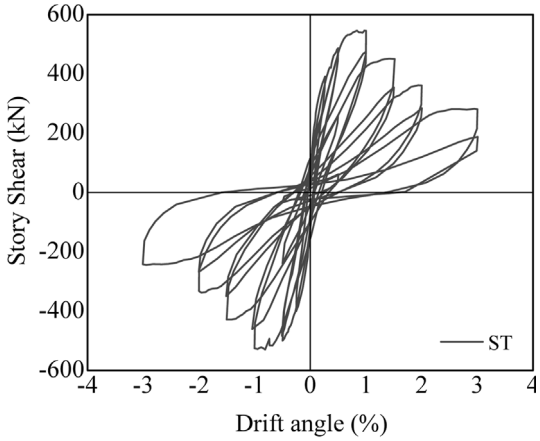

Fig. 9 Story shear vs. drift angle

Photo 1 Crack patterns

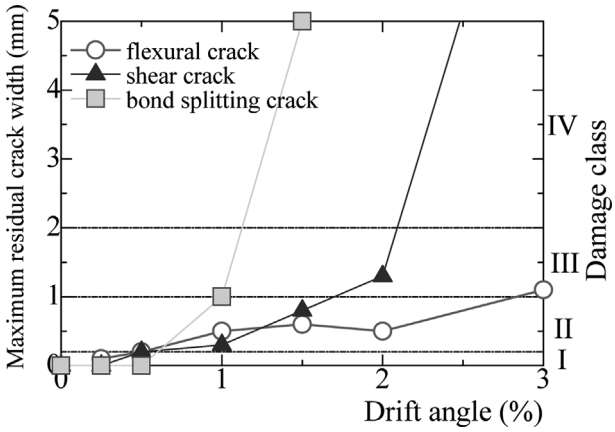

Fig. 10 Maximum crack width vs. drift angle

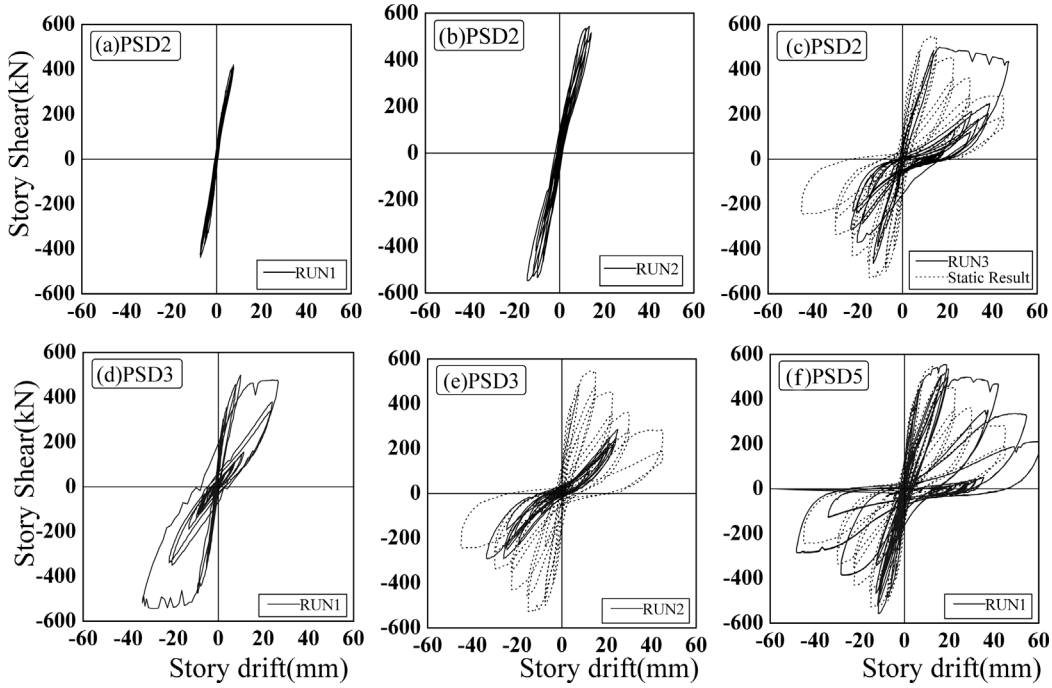

Fig. 11 Relationships between story shear and drift angle

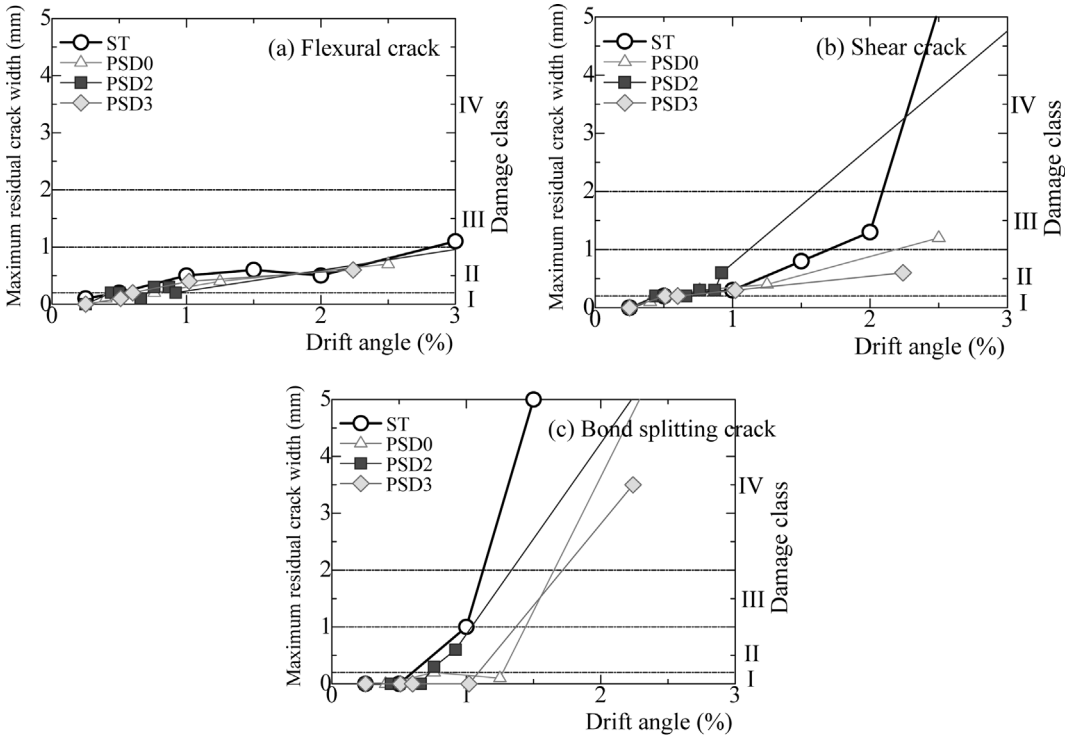

Fig. 12 Maximum residual crack width vs. drift angle

(a) RUN0 of PSD2 (b) RUN0^{+} of PSD2 (c) RUN0 of PSD3

Photo 2 Crack patterns after pre-loading

4.2 Results of pseudo dynamic loading

Fig. 11 shows the observed shear force – lateral displacement relations of specimen PSD0, PSD2 and PSD3. The relationship between the maximum residual crack width and drift angle at the peak of each cycle was shown in Fig. 12. Crack patterns after the pre-loading, RUN0, were shown in Photo 2.

The process to failure was almost similar to the specimens ST. In specimen PSD0 which was subjected to 0.60 time JMA Kobe NS record, after flexural yielding was observed at drift angle of 0.61%, shear force began to decrease with propagation bond splitting cracks and the specimen failed.

Maximum drift angle was 0.5% and maximum residual crack width was 0.2 mm (damage class I) in RUN0 of specimen PSD2, in which amplification factor for the input acceleration was 0.25. In the RUN0^{+} (amplification factor was 0.41), after the specimen yielded at the drift angle of 0.61% and maximum drift angle reached to 1.0% with maximum residual crack width of 0.5 mm (damage class II). In the RUN1 (amplification factor was 0.41), the specimen failed in bond splitting due to rapid increase in drift angle.

Maximum drift angle of 2.24% and bond splitting crack of 3.5 mm width, which was somewhat larger than the criteria of the target damage class III were induced by the RUN0 of specimen PSD3 (amplification factor was 0.50). In the RUN1 with amplification factor of 0.30, shear resistance was deteriorated gradually due to bond splitting failure, although maximum drift angle did not increase markedly.

As can be seen from Fig. 12, no significant difference in residual crack widths between the specimens under static and pseudo-dynamic loading was found.

The relationships between the amplification factor of input acceleration and maximum ductility factors are shown in Fig. 13. In the figure, the lines indicate analytical results for the first story of the 4-degree-of-freedom system and the marks are experimental results. Fig. 13(a) indicates the results without structural damage; i.e., RUN1 for PSD0 and RUN0 for PSD2 and PSD3. Figs. 13(b), (c) and (d) indicate the results after pre-loading. From the figure, maximum ductility response increases with increase in amplification factor of input ground motion. The maximum ductility responses after some damage was induced (Figs. 13(b), (c) and (d)) are generally larger than those without damage. Experimental results approximately agreed well with the analytical results although

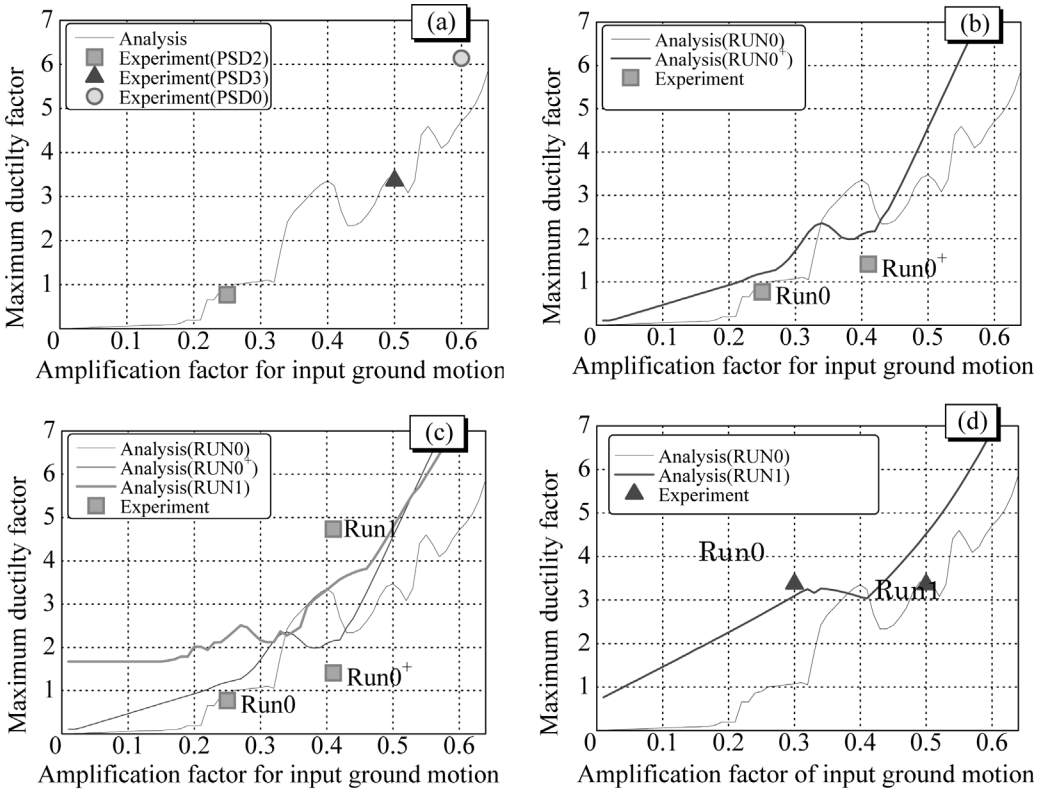

Fig. 13 Relationship between amplification factor of input motion and maximum ductility factor

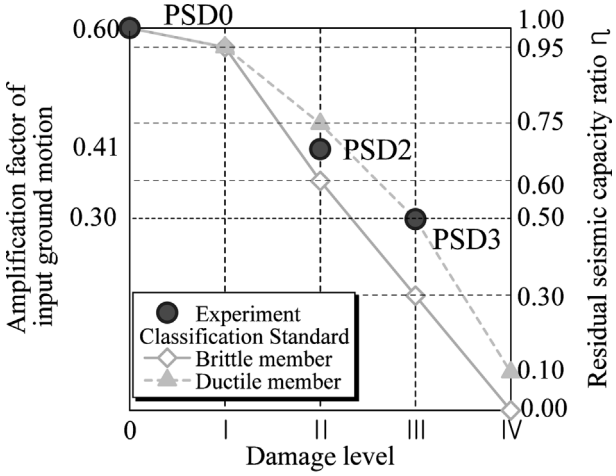

Fig. 14 Comparison of seismic capacity reduction factor η with amplification factor of input ground motion

disagreement can be found for the results of ductility factor of larger than 5 because pinching behavior and deterioration of shear resistance were not taken into account in the hysteresis model for the analyses.

5. Estimation of residual seismic capacity

The seismic capacity reduction factor η of structural members for each damage class is shown in Table 2 based on experimental data of beams and columns under static loading. The basic concept of seismic capacity reduction factor η is illustrated in Fig. 3. Deterioration of seismic capacity was estimated by energy dissipation capacity in lateral force-displacement curve of each member.

To investigate the validity of the seismic capacity reduction factor η in the Guideline, input ground motion levels with which the specimen failed in the pseudo-dynamic testing were compared with the seismic capacity reduction factor in Fig. 14. In the figure, thick line and broken line indicate the seismic capacity reduction factor η for brittle and ductile members respectively. The circles indicate amplification factors of input acceleration in the pseudo-dynamic testing. Amplification factor of 0.60 for undamaged specimen PSD0 was assumed to correspond to the original capacity, $\eta = 1.0$. As can be seen from the figure, amplification factor of 0.41 for RUN1 of PSD2 and 0.30 for RUN1 of PSD3 approximately correspond to the residual seismic capacity ratio η. Accordingly, the proposed the seismic capacity reduction factor η might be useful for the reasonable estimation of post-earthquake seismic capacity of damaged R/C buildings.

6. Conclusions

In this paper, static loading test and sub-structural pseudo-dynamic test of R/C columns were carried out to investigate the validity of the method for post-earthquake capacity evaluation proposed in the Damage Assessment Guideline (JBDPA 2001). From the experimental result, no significant difference in damage levels such as residual crack width between the specimens under static and pseudo-dynamic loading was found. It is shown that the seismic reduction factors η proposed in the Guideline can provide a reasonable estimation of post-earthquake seismic capacity of R/C buildings suffered earthquakes.

References

AIJ/Architectural Institute of Japan (1999), *Standard for Structural Calculation of Reinforced Concrete Structure.* (in Japanese)

Bunno, M. and Maeda, M. (2001), "Post-earthquake damage evaluation for R/C buildings residual seismic capacity in structural members", *The Third US-Japan Workshop on Performance-based Earthquake Engineering for Reinforced Concrete Building Structures*, Seattle.

JBDPA/The Japan Building Disaster Prevention Association (2001), *Standard for Damage Level Classification of Reinforced Concrete Buildings.* (in Japanese)

JBDPA/The Japan Building Disaster Prevention Association (2001b), *Standard for Seismic Evaluation of Existing Reinforced Concrete Buildings.* (in Japanese)

Maeda, M., Nakano, Y. and Lee, K.S. (2001), "Post-earthquake damage evaluation for R/C buildings on residual seismic capacity in structural members", *The 13th World Conf. on Earthquake Engineering*(CD-ROM)

Nakanishi, K., Kitada, T. and Nakai, H. (1999), "Experimental study on ultimate strength and ductility of concrete filled steel columns under strong earthquake", *J. Construct. Steel Res.*, **51**, 297-319.

Nakashima, M. and Masaoka, N. (1999), "Real-time online test for MDOF systems", *Earthq. Eng. Struct. Dyn.*, **28**(4), April, 393-420.

Takeda, T., Sozen, M.A. and Nielsen, N.N. (1970), "Reinforced concrete response to simulated earthquakes", *J. Struct. Div.*, ASCE, **96**(ST12), 2557-2573, Dec.
Taknashi, K. and Nakashima, M. (1987), "A note on the evaluation of damage in steel structures under cyclic loading", *J. Struct. Eng.*, ASCE, **11**(7), 1014-1032.
Usami, T. and Kumar, S. (1996), "Damage evaluation in steel box column by pseudodynamic tests", *J. Struct. Eng.*, ASCE, **122**(6), 635-642.